Exp Brain Res (2014) 232:225–236
DOI 10.1007/s00221-013-3733-8

RESEARCH ARTICLE

Departure from Network Equilibrium (DNE): an efficient and scalable measure of instantaneous network dynamics, with an application to magnetoencephalography

Margaret Y. Mahan · Arthur C. Leuthold · Apostolos P. Georgopoulos

Received: 5 August 2013 / Accepted: 1 October 2013 / Published online: 24 October 2013

Abstract The assessment of the dynamic status of a network is currently unavailable. It is important to know how far a network is away from its equilibrium (as an indicator of instability) at a moment, and over periods of time. Here, we introduce the Departure from Network Equilibrium (DNE), a new measure of instantaneous network dynamics. DNE is simple, fast to compute, and scalable with network size. We present the results of its application on white noise networks (as a basis) and on networks derived from magnetoencephalographic recordings from the human brain.

Keywords Networks · Equilibrium · Scalability · Brain · Magnetoencephalography

Introduction

Networks of interacting elements exhibit global behaviors that cannot be accounted for by the behavior of individual constituent elements but reflect interactions among those elements. One way to measure that global behavior is by obtaining an average of the absolute values of all possible pairwise correlations in the network. Although calculating all possible correlations is in itself a straightforward procedure, it is not scalable to the size of the network, and it quickly becomes intractable, as the number L of pairwise operations (i.e., correlations) increases rapidly with the number K of the network elements (Fig. 1), according to the formula $L = \frac{K!}{(K-2)!2!} = \frac{K\times(K-1)}{2}$. Therefore, a scalable measure of global network behavior would be very desirable. In addition, there are two more points to consider. The first point concerns the kind of information a correlation can provide. This information has to do with the interrelations between constituent elements of the network and not with the global behavior of the network; more specifically, knowledge of all possible pairwise correlations in a network cannot tell us what the status of the network would be at a given instant. The second point concerns the instantaneous assessment of a network's status which is constrained by the minimum sample size (typically about $N = 50$) needed to obtain a correct estimate of a crosscorrelation. Therefore, a measure is needed which would reflect the instantaneous status of the network. In a previous paper (Christopoulos et al. 2012), we introduced such a measure, called "Simultaneous Departure from Equilibrium" (SDE). Assuming that activity of elements in a network would fluctuate randomly above or below their long-term average (element equilibrium), SDE is a normalized logratio of the counts of elements with activities above or below their average, i.e., their equilibrium, at a specific instant. In the work mentioned above (Christopoulos et al. 2012), we defined SDE as the average absolute value of the measure calculated over a period of time. Although this was appropriate for the purposes of that work, namely the assessment of integrated network behavior over a period of many days of recordings in brain cultures, it lacks in two aspects: first, taking the absolute value disregards information concerning the direction of change (above or below equilibrium)

M. Y. Mahan · A. C. Leuthold · A. P. Georgopoulos (✉)
Brain Sciences Center (11B), Department of Veterans Affairs, Minneapolis Health Care System, One Veterans Drive, Minneapolis, MN 55417, USA
e-mail: omega@umn.edu

M. Y. Mahan · A. P. Georgopoulos
Graduate Program in Biomedical Informatics and Computational Biology, University of Minnesota, Minneapolis, MN 55455, USA

A. C. Leuthold · A. P. Georgopoulos
Department of Neuroscience, University of Minnesota Medical School, Minneapolis, MN 55455, USA

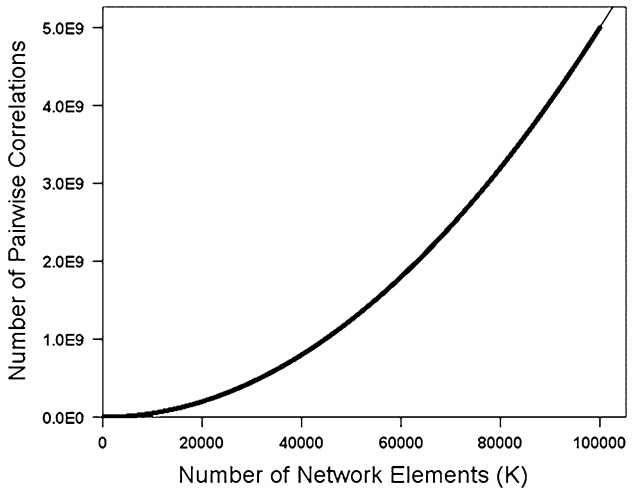

Fig. 1 Non-scalable, explosive increase in the number of pairwise correlations with increasing number of elements in a network

and second, averaging over a period of time disregards information about the instantaneous dynamic status of the network. In fact, SDE can be considered as a derived quantity from the fundamental primary measure of the instantaneous signed logratio of network elements being above or below their equilibrium. In this paper, we analyze in detail this last measure. Since this reflects the instantaneous dynamic status of the network, we call it Departure from Network Equilibrium (DNE), thus placing the emphasis on the equilibrium state of the network, as opposed to that of its elements. The cost for computing this measure increases linearly with K and, hence, avoids combinatorial explosion. In what follows, we investigate DNE time series systematically and extensively using artificial network simulations to derive confidence intervals for DNE distributions and to apply this knowledge to a DNE analysis on brain activity recorded using 248 magnetoencephalographic (MEG) sensors from 169 healthy human subjects. Preliminary data of this work were presented (Georgopoulos and Mahan 2013).

Methods

Calculation of DNE

Consider a network N_m^K consisting of K elements, each of which is a white noise time series Q_t^K of sample size $m(t = 0, 1, 2, \ldots, m)$. An example of a randomly chosen element in a white noise network with $m = 55,000$ is shown in Fig. 2. Specifically, Q_t^K is stationary (Fig. 2a) with values that are also uncorrelated and independent (Fig. 2d), being normally distributed (Fig. 2b, c) with mean zero and constant variance. We further assume that all Q_t^K series are simultaneous, i.e., t is the same for all series. We define A_t and B_t the number of elements of the series Q_t^K that at a given time t have a value above or below their series mean (over m time samples), respectively; if a value equals the mean, it is randomly assigned to the "above" or "below" category. At a given time t, DNE(t) is defined as follows:

$$\mathrm{DNE}(t) = \ln\left\{\frac{\left(\frac{A(t)+1}{B(t)+1}\right)}{(K+1)}\right\} \quad (1)$$

The constant 1 is added to avoid division by zero, and the denominator is a normalizing factor. DNE ranges from -1 to $+1$. Equation (1) is a condensed formula of several equations in Christopoulos et al. (2012).

Statistical analyses

Standard statistical methods were employed using the IBM-SPSS statistical package (version 21) and the Intel FORTRAN/IMSL libraries. The standard error of the cross-correlation was calculated using Bartlett's formula (Bartlett 1978).

Results

DNE of white noise networks

Single white noise networks

In this section, we summarize the results of simulations of networks N_m^K consisting of independent, white noise series. An example of DNE of such a network with $K = 248$, $m = 55,000$ is shown in Fig. 3. It can be seen that DNE is apparently stationary (Fig. 3a) and normally distributed (Fig. 3b), with practically flat autocorrelation function (ACF; Fig. 3c) which remains flat when the DNE values were permuted once (Fig. 3d). The mean of the DNE distribution did not differ significantly from zero (mean $= -0.00001530$, standard error of the mean [SEM] $= 0.000098394$). An important attribute of DNE is its instantaneous magnitude, i.e., how much the network departs from its equilibrium at zero. This information is captured by the standard deviation (SD) of the DNE distribution. We investigated systematically the variation of SD with K (from $K = 10$ to $K = 1,000$, in steps of 10) and m (from $m = 1,000$ to $m = 60,000$, in steps of 1,000). The results are shown in Figs. 4 and 5. It can be seen that SD decreases as a power function of the network size K (Fig. 4). The power function equation was

$$\mathrm{SD} = 1.183K^{-0.708} \quad (2)$$

This relation was highly statistically significant ($r^2 = 0.997$, $F_{[1,98]} = 34,239$, $P < 0.001$). The power function is

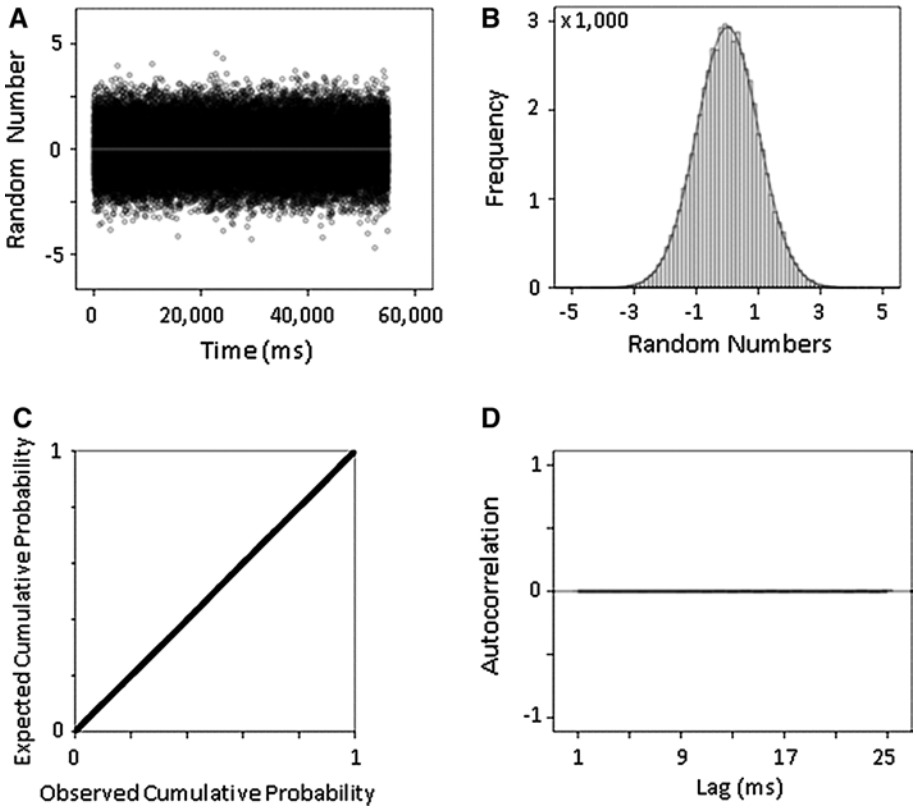

Fig. 2 Attributes of time series of a randomly chosen element in a white noise network. **a** Plot of the time series, **b** histogram of values in **a**, **c** probability–probability plot of the values in **a** to show that the values in **a** are normally distributed, **d** flat autocorrelation function of values in **a** to show that values in **a** are both normally and independently distributed

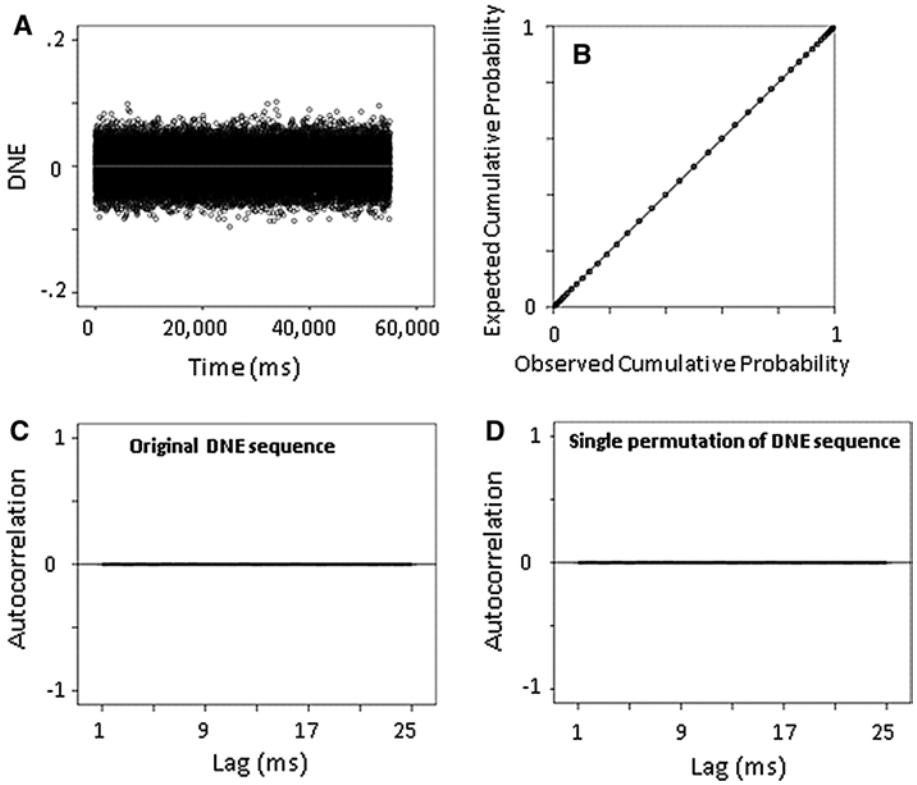

Fig. 3 Attributes of DNE derived from a white noise network ($K = 248$, $N = 55{,}000$). The DNE distribution is apparently stationary (**a**), and symmetrical (**b**). DNEs are independent with flat autocorrelation function (**c**) which remains flat after a single permutation of the time series (**d**)

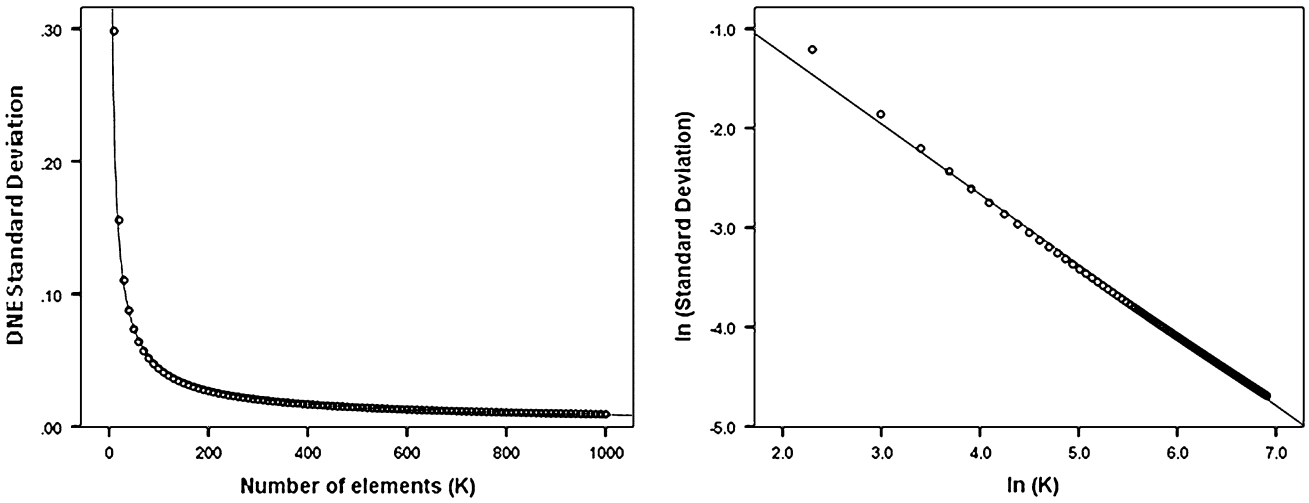

Fig. 4 Dependence of DNE standard deviation on the number of network elements. White noise networks. $N = 60{,}000$. *Left panel*, original scales to illustrate the power fit (see text); *right panel* is the same plot in log–log scales

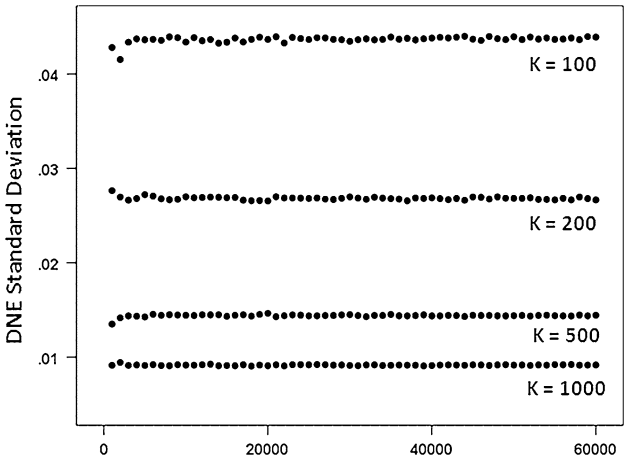

Fig. 5 Independence of DNE standard deviation from the length m of the time series. Notice also the lack of interactions between K and N, as evidenced by the parallel series

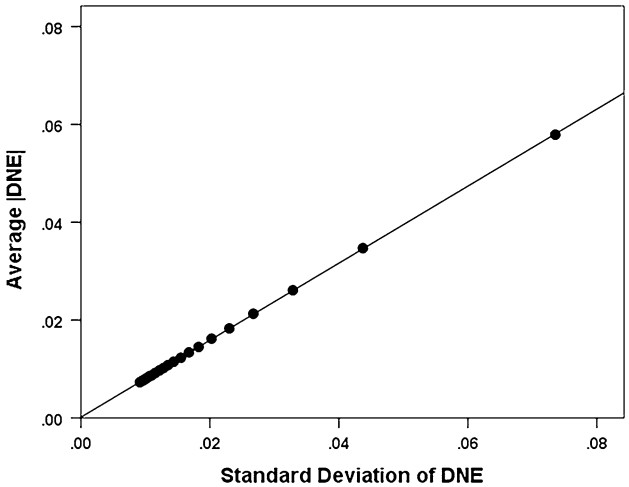

Fig. 6 Perfect association between the average absolute value of DNE and the standard deviation of the signed DNE. Each point ($N = 20$) corresponds to different number of white noise network elements, from 50 to 1,000, every 50

equivalent to a linear dependence of SD on K in a log–log plot, shown in right panel of Fig. 4.

In contrast, SD was independent of time series length m. Figure 5 illustrates the independence of SD from m for different values of K; the same invariance was observed for all K values used. This finding was quantitatively documented by performing an analysis of variance as follows. We generated 60 time series (with length m varying from 1,000 to 60,000, every 1,000) for each of 20 values of K (50–1,000, every 50). We then carried out an analysis of variance for each one of the 20 levels of K, where the SD for each m series was the dependent variable and the time series length m was the independent variable. In all of these analyses, the F statistic was <0.5, with $P \approx 1.0$, thus confirming the independence of SD from m.

These results establish the base for DNE analyses. The SD of the DNE time series is a basic measure for assessing network fluctuations, and an improvement over the mean absolute value used in a previous study (Christopoulos et al. 2012) because of the practically normally distributed DNE (as opposed to the skewed distribution of its absolute value). In addition, the SD contains all the information of the mean (average) |DNE|, as can be appreciated by the practically perfect linear fit in Fig. 6. Twenty white noise DNE distributions of constant time series length

$m = 55,000$ and varying K from 50 to 1,000 every 50 were generated. The SD of the signed DNE values and the average of the absolute DNE values, $|\overline{\text{DNE}}|$, were calculated for each distribution and plotted against each other in Fig. 6. The regression equation obtained was strictly proportional (i.e., the line went through the origin) and of perfect fit $r^2 = 1.0$:

$$|\overline{\text{DNE}}| = 0.787\,\text{SD} \tag{3}$$

This result indicates that the mean |DNE| can be derived from the value of SD without loss of information.

The dependence of the DNE SD on K and its independence from m are both important. The systematic, power function dependence of DNE SD on K establishes a general rule for comparing fluctuations among networks of varying number of constituent elements, in that such a comparison is valid only the K of various networks are taken into account. For example, when the SDs of two networks with different K are to be compared, a new SD calculated from the network with the larger K using random subsets of size K equal to the smaller K would be a valid way to compare the fluctuations of the two networks. On the other hand, the independence of DNE SD on the length of the time series m is an important finding of great practical value for it allows the assessment of network fluctuations based on relatively small series length.

Interacting white noise networks

Consider a pair of networks N_1 and N_2 for which we have their simultaneous DNE time series $\text{DNE}_t^{N_1}$ and $\text{DNE}_t^{N_2}$. We want to explore their interactions, i.e., to find out how one may influence the other and to what extent they may be synchronized. For that purpose, we generated 338 white noise networks with $K = 248$, $m = 55,000$, computed their DNE time series, paired them randomly, and calculated the crosscorrelation function between DNEs of the resulting 169 pairs. Crosscorrelation functions were practically flat; an example is shown in Fig. 7. Considering the crosscorrelation at zero lag, there were only 3 values that exceeded a t-statistic threshold of 2 (absolute value of crosscorrelation over its standard error, calculated using Bartlett's (1978) formula; $P < 0.05$); by chance, one would have expected up to 5 % of values (~8 of 169) to exceed that threshold. These findings indicate that, as expected, DNEs of white noise networks are not associated by chance.

DNE of MEG networks

Single MEG networks and comparison with white noise networks

The data used in these analyses consisted of continuous 55,000 time samples of MEG recordings from 248 axial

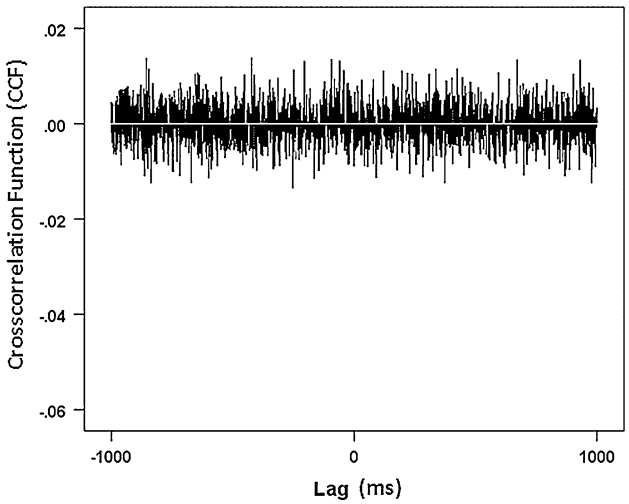

Fig. 7 Lack of interactions between white noise networks, as evidenced by this example of an essentially flat crosscorrelation function (maximum lag ±1,000 ms. $K = 248$, $N = 55,000$ for each of the two crosscorrelated white noise networks)

gradiometers sampled at 1,017 Hz during a task-free state from 169 cognitively healthy women (MoCA ≥ 26; Montreal Cognitive Assessment: http://www.mocatest.org/). MEG acquisition details are given in Leuthold et al. (2013). Each dataset (of the 169) consisted of 248 time series resulting in a rectangular 55,000 × 248 matrix of recorded MEG signal. Each time series was prewhitened using a Box–Jenkins (Box and Jenkins 1970) AutoRegressive Integrated Moving Average (ARIMA) model with autoregressive (p), differencing (d), and moving average (q) orders of $p = 50$, $d = 1$, $q = 1$ to make the series stationary and eliminate internal dependencies. The resulting innovations (residuals) were practically white noise. An example is shown in Fig. 8 where the innovations of a single MEG time series (i.e., from one sensor) and some of attributes are plotted. It can be seen that the series is stationary (Fig. 8a), the values of the series are normally distributed (Fig. 8b, c), and their autocorrelation function is flat (Fig. 8d). One hundred and sixty-nine MEG networks were thus available with $K = 244 - 248$ and $m = 55,000$. The number of valid sensors (i.e., K) varied in different subjects, due to hardware reasons at the time of recording; $K = 248$ in 81 subjects, $K = 247$ in 81, and $K = 246$ in 7 subjects. For comparisons with white noise networks (see below), such networks were generated using K values as the distribution above; e.g., 81 white noise networks were generated with $K = 248$, 81 networks with $K = 247$, and 7 with $K = 246$. DNE data for one such network are shown in Fig. 9. It can be seen that the DNE time series is apparently stationary (Fig. 9a) and normally distributed (Fig. 9b). However, its autocorrelation function is not flat but shows a clear autoregressive structure (Fig. 9c). This structure is due to the

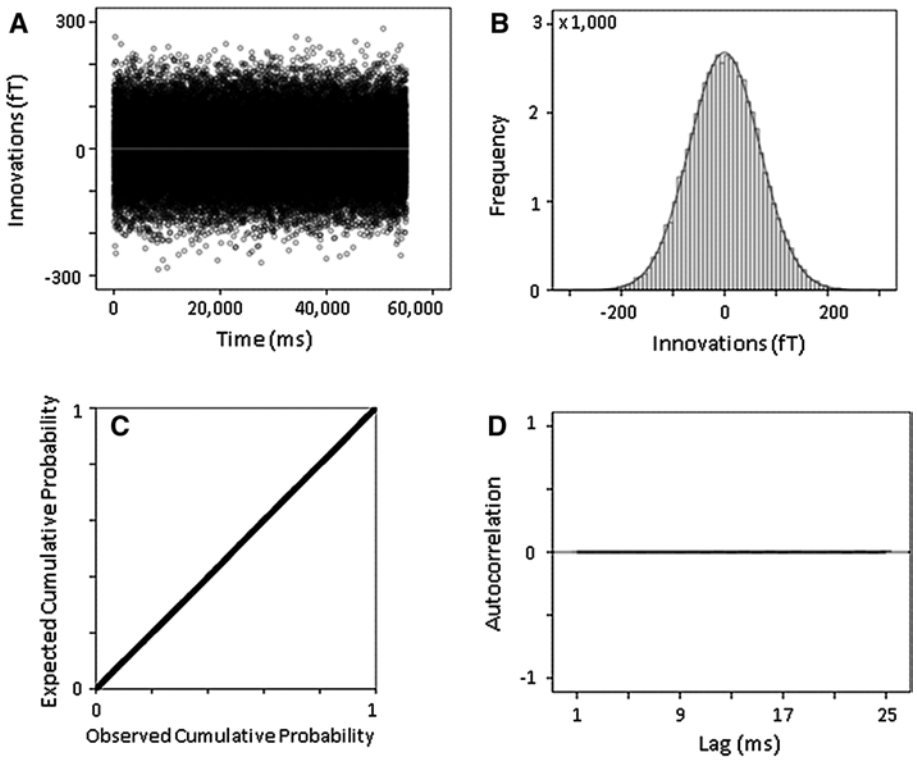

Fig. 8 Attributes of a prewhitened MEG time series. Innovations from ARIMA (50, 1, 1) are normally distributed and independent. Plots as in Fig. 2

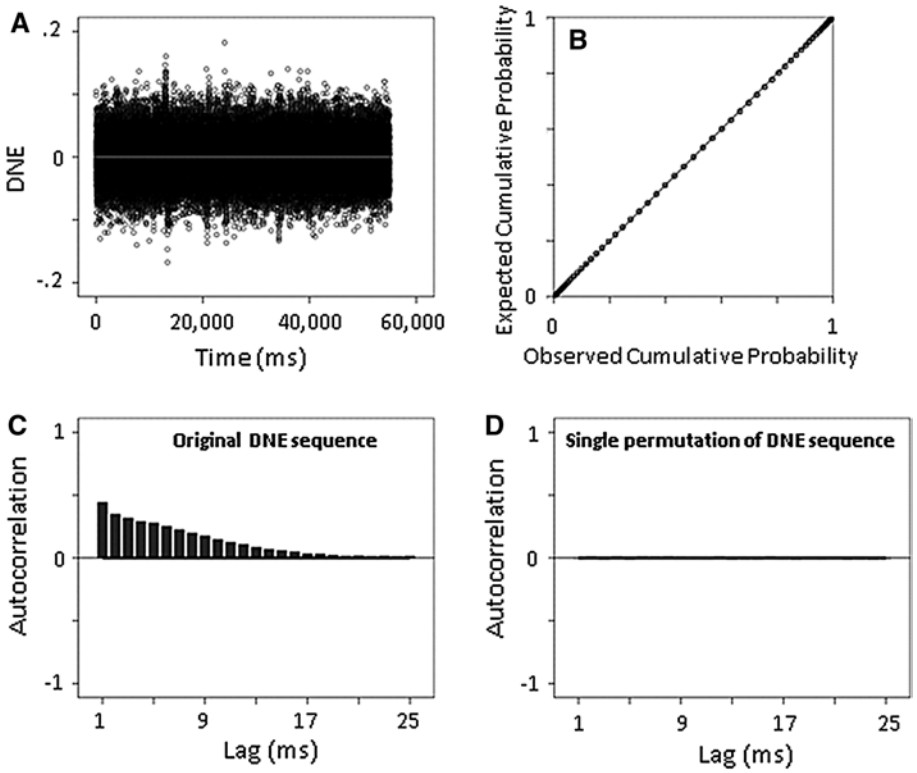

Fig. 9 Attributes of MEG DNE obtained from MEG innovations. The DNE series are apparently stationary (**a**) and symmetrically distributed (**b**). However, they are not independent, as evidenced by the systematic autocorrelation function (**c**). This autoregressive dependence is abolished by a single permutation of the DNE series (time shuffling, **d**)

temporal sequence of DNE values since it disappeared after a single random shuffling (permutation) of the time series (Fig. 9d).

We examined in more detail the mean, spread, and autocorrelation function of the DNE distributions. These are crucial attributes, since (a) the mean indicates the

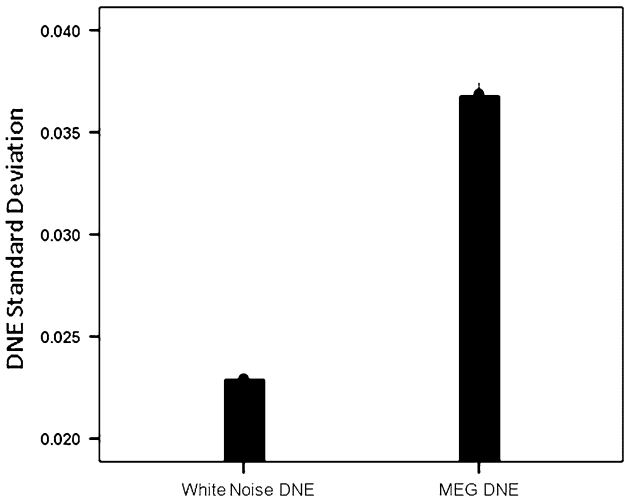

Fig. 10 The standard deviation of the MEG DNEs is significantly larger than that of white noise DNEs. (See text for details)

long-term average of DNE, i.e., the center of its equilibrium, (b) the spread (e.g., standard deviation) is a measure of network excursions away from its average (equilibrium point), and (c) the autocorrelation function is informative about the internal dependencies between successive DNE values of the network. We found the following. First, none of the means of the DNE of all 169 MEG and 169 white noise networks differed significantly from zero. This indicates that indeed the equilibrium point of the DNE distribution is at zero. Second, the SDs of the DNE of the MEG networks were larger than those of the white noise networks (Fig. 10) (mean ± SEM: $SD_{MEG} = 0.0376 \pm 0.000606$ versus $SD_{random} = 0.0231 \pm 0.0000061$, paired $t_{129} = 24.0$, $P < 0.001$). This indicates that the brain networks show larger departures from their equilibrium than the white noise networks. And third, all MEG DNE distributions showed a strong autocorrelation structure, as illustrated in the example of Fig. 9c. This necessitated an exploration of the various possible internal dependencies of the DNE time series (model identification). First, we ensured that the series are stationary by detailed inspection of the series itself and by calculating the mean and variance of consecutive time bins; those steps did not produce evidence of non-stationarity. In addition, we applied a (0, 1, 0) ARIMA model (i.e., only differencing the series) and compared the normalized Schwarz's Bayesian criterion (Schwarz 1978) between the original and the differenced series; there was no appreciable or systematic reduction in these measures after differencing, which suggests that the series were indeed stationary. The autocorrelation structure suggests an autoregressive process which extends about 25 ms back. Using this approximate estimate as a first step, we applied a (25, 0, 0) ARIMA model and examined the resulting innovations. We found that those innovations had flat autocorrelation and partial autocorrelation functions, i.e., they were practically like white noise. Moreover, the addition of a moving average component to the model, now (25, 0, 1), did not improve the normalized Schwarz's Bayesian criterion and did not yield a statistically significant moving average coefficient. These results indicated that the MEG DNE process is a pure autoregressive process.

In contrast to the results above, none of the white noise DNE networks showed any internal dependencies, as evidenced by their flat autocorrelation function (Fig. 3c). Nevertheless, we performed an additional analysis to test the hypothesis that the autoregressive structure of the MEG DNE network series is exclusively due to the temporal sequence of the DNE values. For that purpose, we shuffled once each one of the 169 MEG DNE time series and recomputed their autocorrelation function. We found that they all became flat, the same as illustrated in Fig. 9d, which proved our hypothesis correct.

These findings document the fundamentally different temporal structure of MEG DNEs from white noise DNEs. The main difference lies in the autoregressive dependence in the former DNEs, typically back to 25 ms. The practical significance of this property lies in the need for MEG DNE time series to be prewhitened when interactions between them are evaluated (see below). In fact, as shown above, a pure autoregressive ARIMA model of (25, 0, 0) is adequate to accomplish this goal. This paved the way for assessing the interactions between biologically meaningful MEG DNE networks, as described below.

Interacting MEG networks

There are two points to be stressed before we proceed with the details of this analysis. First, there were no significant interactions between white noise DNE networks (see above). And second, given their autoregressive dependency of the MEG DNE time series, they were prewhitened before analyzing their interactions. This was achieved by applying a (25, 0, 0) ARIMA model which yielded practically white noise innovations. Given the high-frequency (1,017 Hz) sampling of the MEG signal, and the prewhitening of the series (i.e., removing low-frequency components in the individual series), it is reasonable to assume that the MEG signal used for the analysis came from weak magnetic sources, in the vicinity of the MEG sensors (see Engdahl et al. 2010 for further discussion of this point). We carried out analyses of the interactions between DNEs from three brain sites: (a) interhemispheric interactions by assessing the interactions between left and right hemispheric DNEs, (b) intra-hemispheric interactions between arbitrary networks within the left hemisphere, and (c)

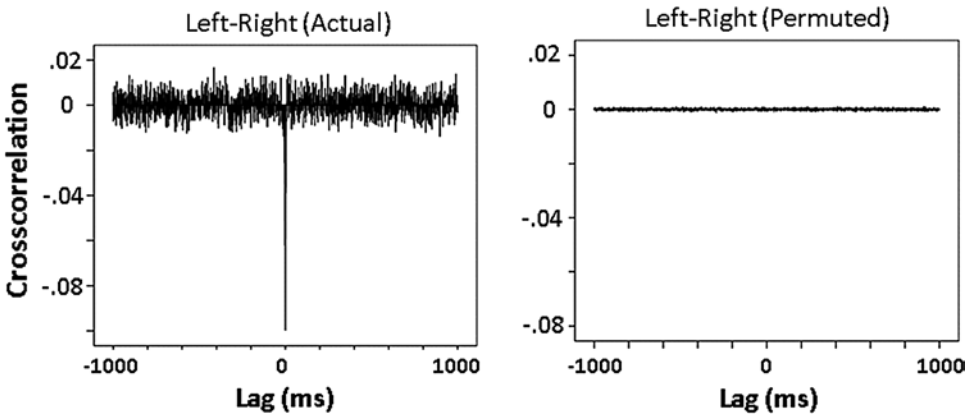

Fig. 11 An example of negative zero-lag crosscorrelation between left and right hemispheric DNE networks in a single subject (*left panel*). This correlation is abolished by a single random permutation of the series (*right panel*), attesting to the precise temporal structure underlying this interaction

intra-hemispheric interactions between arbitrary networks within the right hemisphere. We found the following.

Interhemispheric (left–right) DNE interactions

The left and right hemisphere networks consisted of $K = 116$ sensors each. (Sixteen sensors were excluded from this analysis because they were located on the midline.) We computed two DNE time series for each subject, one for the left and the other for the right hemisphere. They were prewhitened using a (25,0,0) ARIMA model and the crosscorrelation function was computed with maximum lag of ±1,000 ms. In parallel, we computed DNEs of white noise networks with $K = 116$. Preliminary inspection of the crosscorrelation functions of the 169 individual left–right brain DNEs revealed large zero-lag crosscorrelations. An example is shown in the left panel of Fig. 11. The correlation disappears after a single permutation of the time series (Fig. 11, right panel) which documents the dependence of the correlation on the temporal structure of the two series. In contrast, all DNEs from white noise networks were flat (data not shown). All 169 zero-lag crosscorrelations were highly statistically significant ($P < 0.001$), and most of them (127/169 = 75.1 %) were negative (see histogram in Fig. 12).

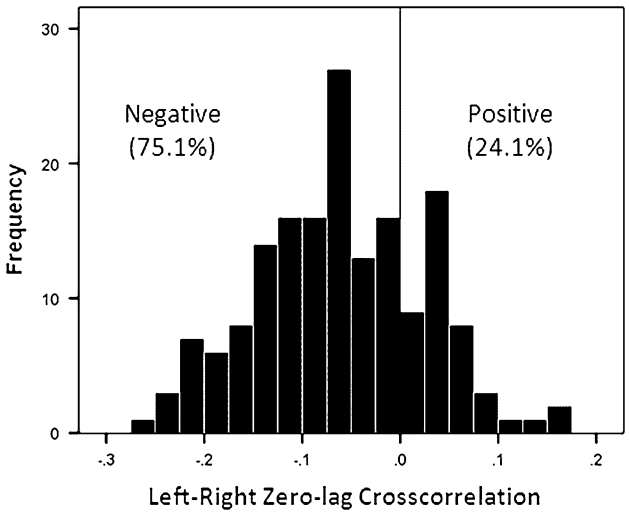

Fig. 12 Frequency distribution of zero-lag crosscorrelations between left and right MEG DNE series. Most of the correlations (75 %) are negative

Intrahemispheric (within hemisphere) DNE interactions

In contrast, network interactions within a hemisphere were characterized by strong zero-lag positive correlations. Since intrahemispheric networks are not unique, we carried out 10 random crosscorrelation analyses per hemisphere, as follows. There were 116 MEG sensors available per hemisphere, so we assigned randomly 58 to each of 2 networks, and then calculated respective DNE and calculated their zero-lag crosscorrelation, as described above. We repeated this procedures 10 times for each subject and hemisphere, for a total of 10 × 169 = 1,690 crosscorrelation values per hemisphere. Examples of single (out of the 10 random) within-left and within-right crosscorrelation functions from one subject are shown in Fig. 13, together with the left–right crosscorrelation function. Figure 14 plots histograms of all 1,690 within-left and within-right hemisphere crosscorrelations, and Fig. 15 shows that those were correlated between themselves. With respect to left hemisphere, all but one crosscorrelation values were positive; for the right hemisphere, all values were positive. Overall, crosscorrelation values were significantly higher in the right than the left hemisphere (Kolmogorov–Smirnov test, $P < 0.001$; left crosscorrelation median = 0.256, right crosscorrelation median = 0.286), and both within-left and within-right hemisphere correlations were stronger than the interhemispheric ones (median of absolute value of left–right crosscorrelation = 0.0717). Finally, the correlation between MEG DNE networks did not depend on the number K of elements in the network ($P = 0.396$; z-transformed zero-lag correlations between two DNE networks of sizes

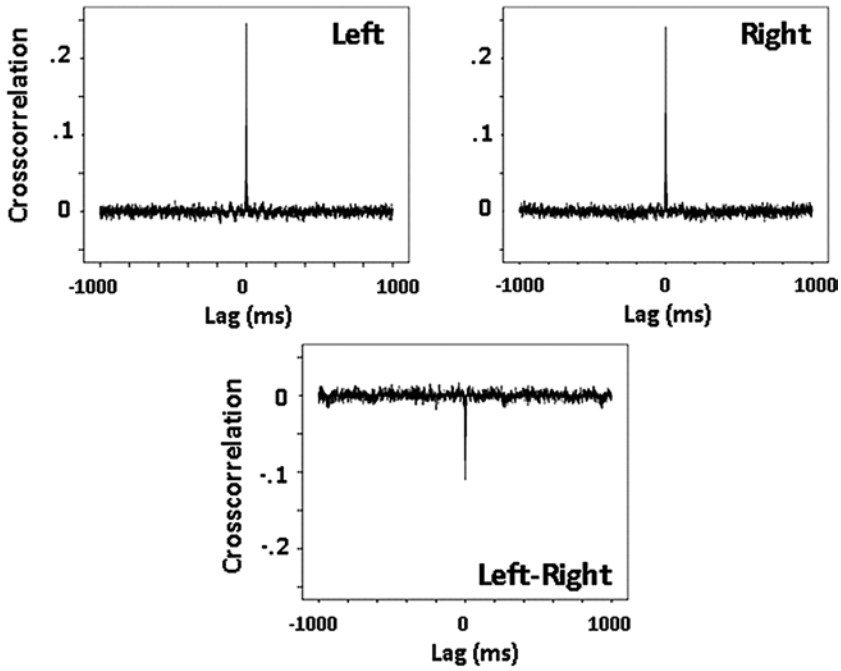

Fig. 13 Strong positive zero-lag correlations obtained between two random MEG DNE from within the left and right hemispheres (*top panel*), contrasted to a negative zero-lag correlation between the left and right hemisphere (*lower panel*). All data are from one and the same subject

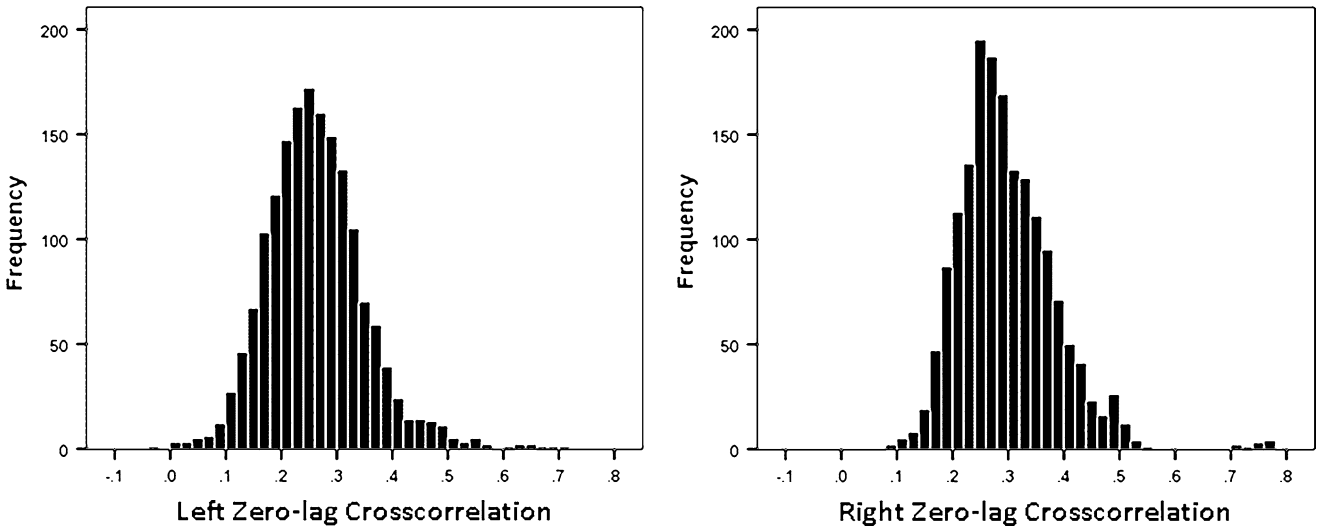

Fig. 14 Frequency distributions of zero-lag correlations between 10 pairs of randomly chosen MEG DNE networks for the left and right hemispheres. $N = 1{,}690$ values per plot (169 subjects × 10 runs per subject; see text for details)

$K_1 = K_2 = 20, 25, 30, 35, 40, 45, 50, 55$ regressed against network size).

Effects of age and handedness on DNE interactions

To investigate this question, we transformed individual zero-lag crosscorrelation (r) values using Fisher's z-transformation (Fisher 1958):

$$z = \frac{\log_e\left(\frac{1+r}{1-r}\right)}{2} \tag{4}$$

Interhemispheric left–right z values (z_{LR}) were retained for each of the 169 subjects; z values for the within-left (z_L) and within-right (z_R) hemispheres were averaged across the 10 random runs for each hemisphere. Thus, for each subject, z-transformed zero-lag correlations were available for the interhemispheric and the within-left and within-right hemisphere case. The dependence of these correlations upon age (Fig. 16) and/or handedness (Fig. 17) was evaluated using a linear regression model, where the z value was the dependent variable and age and/or handedness were the independent variables. We found the following.

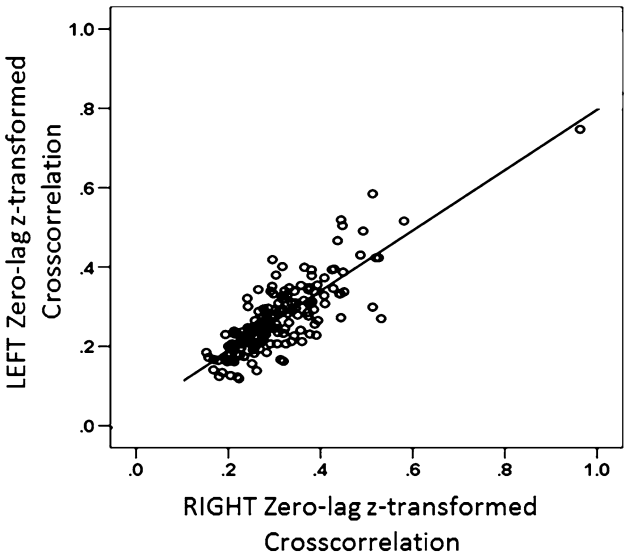

Fig. 15 High congruence between the strength of zero-lag crosscorrelations from left and right hemispheres. Data plotted are *z*-transformed correlations (Fisher 1958). This strong relation was practically unchanged when the single high point was removed from the analysis. The fitted line lies below the diagonal because the values in the right hemisphere are higher than those in the left hemisphere

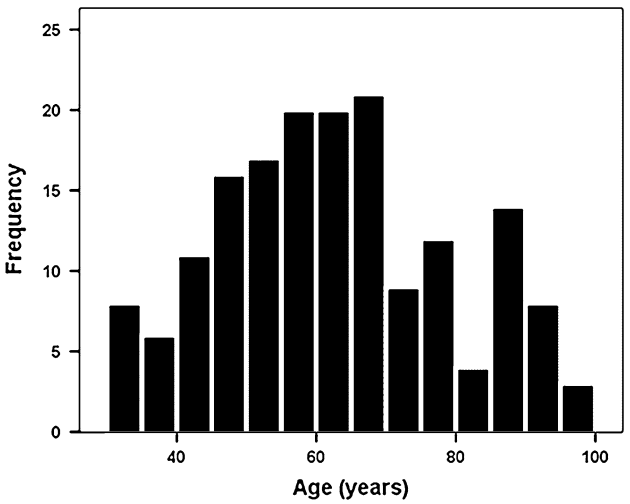

Fig. 16 Frequency distribution of ages of the 169 subjects of the study

The interhemispheric z_{LR} was affected significantly by both age and handedness, according to the following equation:

$$z_{LR} = -0.163 + 0.001973A - 0.000299H \quad (5)$$

where A is the age in years (in decimal fractions) and H is the Edinburgh handedness score (Oldfield 1971). Both effects were statistically significant, although the effect of age was more highly significant ($P < 0.0001$) than that

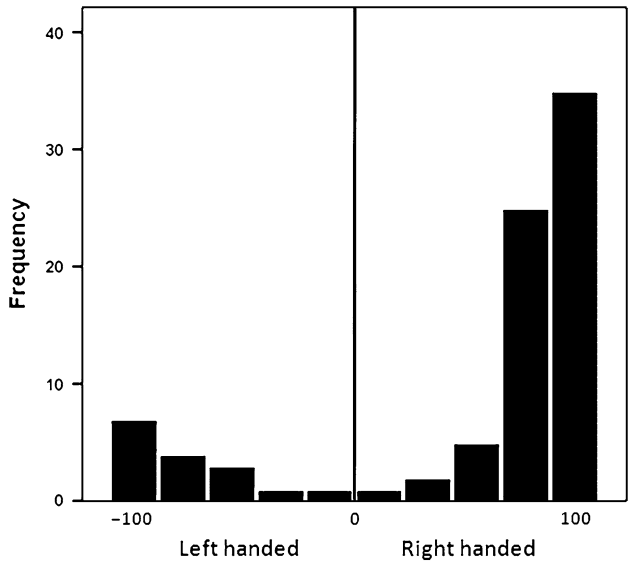

Fig. 17 Frequency distribution of the Edinburgh handedness score of the 169 study subjects

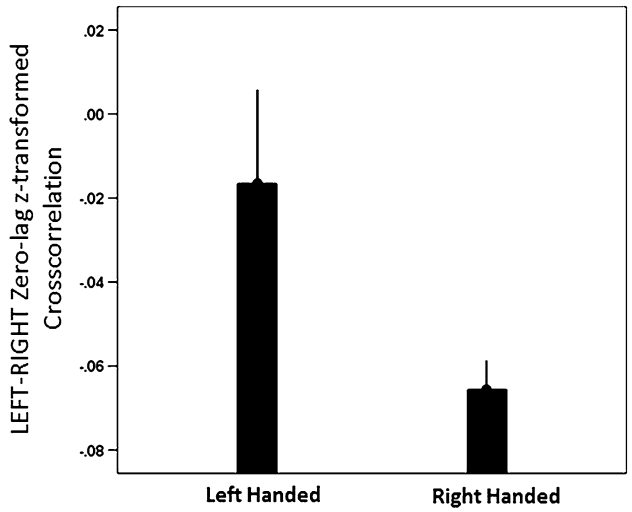

Fig. 18 Zero-lag crosscorrelations between the left and right MEG DNE series differ significantly between left- and right-handed subjects; they are higher in the left-handed subjects

for handedness ($P = 0.014$). The effect of handedness was stronger in the left-handed subjects (Fig. 18). Finally, these effects were independent of each other, since a multiplicative $A \times H$ interaction term was not statistically significant when entered in Eq. 5 above ($P = 0.765$).

The within-right hemisphere correlations were independent of either age ($P = 0.651$) or handedness ($P = 0.743$). However, the within-left hemisphere correlations were significantly affected by age ($P = 0.004$) but not handedness ($P = 0.276$). The equation was

$$z_L = 0.348 - 0.001221A \quad (6)$$

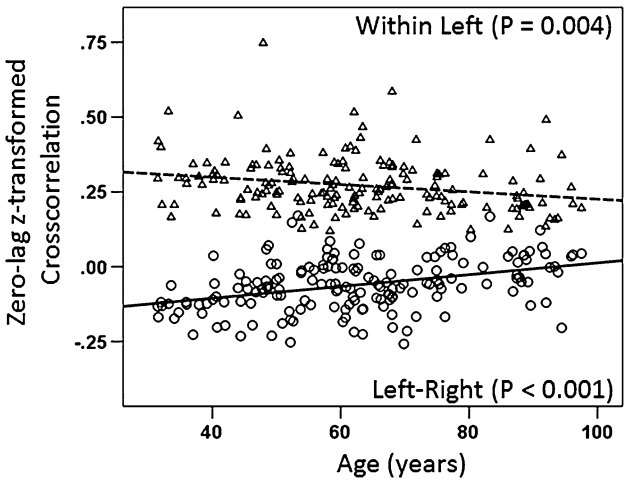

Fig. 19 Decorrelation of interactions between MEG DNEs with increasing age: the left–right interactions tend to become less negative (*open circles*), and the within-left hemisphere interactions tend to become less positive (*open triangles*). $N = 169$ subjects per cloud. See text for details

Discussion

The above results are based on a relatively large sample ($N = 169$) of cognitively healthy women and provide new insights into the dynamic interactions between cortical networks and their relations to age and handedness. With respect to interhemispheric interactions, the issue has been studied and discussed extensively (for reviews, see Doron et al. 2012; Fling et al. 2011). Our results are in accord with previous findings that functional hemispheric asymmetry is reduced with age (Fling et al. 2011). In addition, we documented an independent effect of handedness such that increasing right handedness was associated with increasing interhemispheric negative correlation. These results underscore the importance of taking into account of both age and handedness in studies of interhemispheric interactions. On the other hand, since our study population comprised only women, we cannot make any statements concerning gender differences and their potential interactions with age and handedness. Finally, our finding of stronger interhemispheric correlations in left-handed subjects is in accord with the reported more efficient hemispheric interactions in an interhemispheric transfer time task (Cherbuin and Brinkman 2006).

With respect to functional interactions within each hemisphere, our results were surprising in that they revealed fundamental similarities and differences between the two hemispheres. Specifically, network interactions within both hemispheres were strongly positive and independent of handedness but in the left hemisphere the positive correlation decreased significantly with age. Overall, the absolute value of the zero-lag crosscorrelation decreased with age both between hemispheres and within the left hemisphere (Fig. 19). Altogether, these findings indicate an increasing decorrelation in network interaction with increasing age. The importance of neural network decorrelation in information processing has been pointed out by several investigators, mostly in the context of visual processing (Dimitrov and Cowan 1998; Daugman 1989; Vinje and Gallant 2000; Pitkow and Meister 2012) and neural network modeling (Rosen 1996). In a way, network decorrelation can be regarded as a mechanism by which the network is "freed" from the hold of a particular input (e.g., sensory stimulus or a life event) and becomes available for encoding new information. Thus, older brains may become more efficient information processors, commonly thought of as maturity or wisdom. Interestingly, a neural decorrelation mechanism has been described recently with respect to resilience to trauma (James et al. 2013).

Conclusions

The DNE approach possesses a major advantage over pairwise or higher-order correlations, namely that it is a much simpler measure and one that is very easy and fast to compute. In addition, the DNE measure opens new avenues in analyzing and assessing network function at different levels of organization and time scale, both for descriptive purposes as well as for the purpose of assessing effects of interventions on network function. Finally, this approach is fairly general and can be formally extended to any network (neural or not), with potentially useful applications to econometric, social, geoscience, and other networks.

Acknowledgments This work was supported by the American Legion Brain Sciences Chair. This material is based upon work partially supported by the National Science Foundation under Grant No. 00006595. Any opinions, findings, and conclusions or recommendations expressed in this material are those of the authors and do not necessarily reflect the views of the National Science Foundation.

References

Bartlett MS (1978) An introduction to stochastic processes with special reference to methods and applications, 3rd edn. Cambridge University Press, Cambridge, MA

Box GEP, Jenkins GM (1970) Time series analysis: forecasting and control. Holden Day, San Francisco, CA

Cherbuin N, Brinkman C (2006) Hemispheric interactions are different in left-handed individuals. Neuropsychology 20:700–707. doi:10.1037/0894-4105.20.6.700

Christopoulos VN, Boeff DV, Evans CD, Crowe DA, Amirikian B, Georgopoulos A, Georgopoulos AP (2012) A network analysis of developing brain cultures. J Neural Eng 9:046008-2560/9/4/046008. doi:10.1088/1741-2560/9/4/046008

Daugman JG (1989) Entropy reduction and decorrelation in visual coding by oriented neural receptive fields. IEEE Trans Biomed Eng 1:107–114

Dimitrov A, Cowan JD (1998) Spatial decorrelation in orientation-selective cortical cells. Neural Comput 10:1779–1795

Doron KW, Bassett DS, Gazzaniga MS (2012) Dynamic network structure of interhemispheric coordination. Proc Natl Acad Sci USA 109:18661–18668. doi:10.1073/pnas.1216402109

Engdahl B et al (2010) Post-traumatic stress disorder: a right temporal lobe syndrome? J Neural Eng 7:066005

Fisher RA (1958) Statistical methods for research workers, 13th edn. Oliver and Boyd, Edinburgh

Fling BW, Peltier SJ, Bo J, Welsh RC, Seidler RD (2011) Age differences in interhemispheric interactions: callosal structure, physiological function, and behavior. Front Neurosci 5:38. doi:10.3389/fnins.2011.00038

Georgopoulos AP, Mahan MY (2013) Simultaneous Departure from Equilibrium (SDE): an efficient measure of dynamic interactions in massively interconnected networks. In: Annual symposium on biomedical informatics and computational biology, Jan 18, Rochester, MN

James LM, Engdahl BE, Leuthold AC, Lewis SM, Van Kampen E, Georgopoulos AP (2013) Neural network modulation by trauma as a marker of resilience: differences between veterans with post-traumatic stress disorder and resilient controls. JAMA Psychiatry 70:410–418

Leuthold AC, Mahan MY, Stanwyck JJ, Georgopoulos A, Georgopoulos AP (2013) The number of cysteine residues per mole in apolipoprotein E affects systematically synchronous neural interactions in women's healthy brains. Exp Brain Res 226:525–536. doi:10.1007/s00221-013-3464-x

Oldfield RC (1971) The assessment and analysis of handedness: the Edinburgh inventory. Neuropsychologia 9:97–113

Pitkow X, Meister M (2012) Decorrelation and efficient coding by retinal ganglion cells. Nat Neurosci 15:628–635

Rosen BE (1996) Ensemble learning using decorrelated neural networks. Connect Sci 8:373–384

Schwarz GE (1978) Estimating the dimension of a model. Ann Stat 6:461–464. doi:10.1214/aos/1176344136

Vinje WE, Gallant JL (2000) Sparse coding and decorrelation in primary visual cortex during natural vision. Science 287:1273–1276